

ARTICLES

Up-converted luminescence and excited-state excitation spectroscopy of Cr^{4+} ions in forsterite

S. G. Demos, V. Petričević, and R. R. Alfano

*Institute for Ultrafast Spectroscopy and Lasers, Department of Physics, The City College
and Graduate School of the City University of New York, New York, New York, 10031*

(Received 13 February 1995)

The electronic structure of Cr^{4+} -doped forsterite is studied using up-converted luminescence and excited-state excitation spectroscopy. Two metastable states with energies higher than the energy of the 3T_2 lasing level are identified. The first, higher-lying state was identified as ${}^3T_1(t_2e)$ electronic state. Three lines were resolved at 26 424, 26 529, and 26 625 cm^{-1} , corresponding to the spin-orbit-split zero-phonon line of the ${}^3T_1(t_2e)$ state. The lifetime of this state was measured to be 395 ps. The second, lower-lying state is located at $12\,847 \pm 90 \text{ cm}^{-1}$ and is assigned to the ${}^3T_1(t_2^2)$ state. Its lifetime is estimated to be of the order of a few hundred nanoseconds.

INTRODUCTION

The discovery and subsequent development of chromium-doped forsterite ($\text{Cr}:\text{Mg}_2\text{SiO}_4$) as an important tunable solid-state laser tunable between 1150 and 1350 nm have generated considerable interest in obtaining information on the basic properties of this material.¹⁻⁵ The unique spectroscopic property of chromium-doped forsterite is that the tetravalent chromium (Cr^{4+}) substituting for tetrahedrally coordinated Si^{4+} was identified as the lasing center.^{2,3,6-10} The electronic structure of forsterite has been studied by absorption and emission measurements⁶⁻⁹ as well as electron paramagnetic resonance.¹⁰ These measurements clearly demonstrate the presence of both Cr^{3+} and Cr^{4+} ions in forsterite. The dominant emission reported is the transition from the lowest excited electronic state (3T_2) to the ground state (3A_2) of the Cr^{4+} ions. In this paper, we investigate the upper electronic state structure of the Cr-doped forsterite using up-converted luminescence and excited-state excitation spectroscopy.

The term up-converted luminescence describes the emission from higher excited electronic states populated by excited-state absorption (ESA). The up-converted emission is blueshifted with respect to the excitation laser wavelength. In forsterite, the lowest vibronic level of the spin-orbit split storage level (SL) is located at 9137 cm^{-1} (3T_2 electronic state). The lifetime of the SL is 25 μs at a temperature of 77 K and decreases to 2.7 μs at room temperature. Two additional metastable levels with higher energy than the energy of the lasing level in the electronic structure of the Cr^{4+} ion in forsterite have been identified in this work. This conclusion was arrived at by studying the spectral characteristics of the up-converted luminescence. The existence of the higher-lying metastable state was confirmed by excited-state excitation measurements.

There are two types of emission associated with radiative transition from the excited states. These are the ordinary luminescence (OL) and the hot luminescence (HL). The OL emission arises from transitions between metastable levels and the ground state. The HL emission is due to radiative transitions from the manifold of non-equilibrium vibronic states populated during the nonradiative decay.¹¹⁻¹⁴ The fundamental difference between OL and HL is that OL is independent of the pumping wavelength since it depends only on the position of the metastable level. On the other hand, HL occurs immediately after photoexcitation and the emission starts from the laser excitation wavelength. In the case of up-converted luminescence, both types of emission are possible. The first type (up-converted OL) has been extensively studied in rare-earth ion-doped crystals due to their potential use as up-conversion lasers.^{15,16} In transition-metal-doped materials, up-converted OL was first reported in $\text{MgF}_2:\text{Ni}^{2+}$.¹⁷ Using a very sensitive photodetector, up-converted OL and HL (Ref. 18) were observed in forsterite.

EXPERIMENTAL METHOD

The sample was photoexcited by a synchronously pumped dye laser and the 532-nm second harmonic of a cw mode-locked Nd:YAG (neodymium-doped yttrium aluminum garnet) laser. Using different dyes, the excitation laser wavelength was tuned from 573 to 790 nm. The laser power was 300–600 mW depending on the wavelength. The laser beam was focused into the sample by a 10-cm focal-length lens. The backscattered light was collected by an 85-mm camera lens and spectrally analyzed by a SPEX triplemate spectrograph. The detector was an ultrasensitive Hamamatsu Photon Counting Image Acquisition System (PIAS). The sample was a Cr-doped forsterite crystal with a dopant concentration of 0.02 at. % of Cr. All experiments were carried out with

the sample held at liquid-nitrogen temperature.

The use of ultrashort, low-energy pulsed-laser excitation requires that the two photons involved in the overall photoexcitation, the first to reach the SL and the second for ESA, belong to different pulses. This means that ESA is possible when the lifetime of the SL is longer than the time interval between consecutive pump pulses (12 ns in our experiments).

The ESA process involves the absorption of a photon while the ion is in the excited state to reach an excitation level with energy (E_{EL}) given by

$$E_{EL} = E_{ph} + E_{SL}, \quad (1)$$

where E_{ph} is the photon energy, and E_{SL} is the average energy of the SL (3T_2) $E_{SL} = 9150 \text{ cm}^{-1}$. Subsequently to the two-step photoexcitation, the metastable levels located below the excitation level will be populated through nonradiative relaxation of the ions. This process is depicted in Fig. 1. Three metastable levels are displayed, and the two-step photoexcitation process is depicted for three different laser wavelengths. Photoexcitation of the Cr^{4+} ions populates the lower-lying metastable levels. Excited-state absorption from these levels leads to the population of the higher-lying metastable level. Up-converted OL occurs from the radiative transitions between the metastable levels populated by ESA and the ground state. Varying the laser wavelength and monitoring the up-converted luminescence, information was obtained on the position of the metastable levels. Details regarding Fig. 1 are described below.

The two-step photoexcitation process was used to measure the excited-state excitation spectrum of the Cr^{4+} ion in the violet and near-ultraviolet spectral region. In this case, the integrated luminescence intensity over the 370–410-nm range was measured as the excitation wavelength was changed from 572.7–594.5 nm, which, assuming a two-step process, resulted in effective excitation from 25 970–26 610 cm^{-1} . This method enabled us to

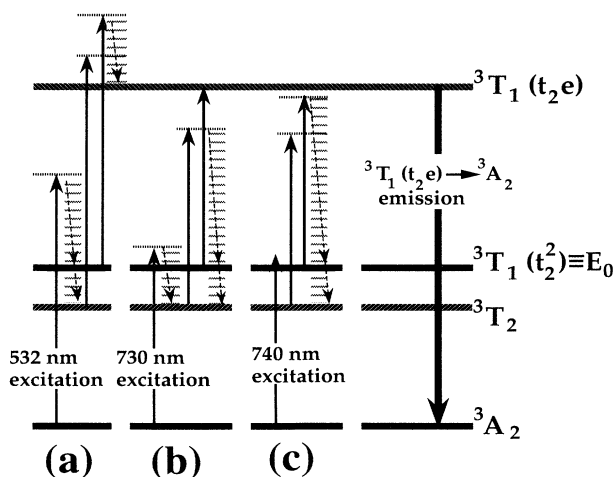


FIG. 1. Schematic diagram showing the up-converted ordinary luminescence process in Cr^{4+} forsterite under (a) 532-nm, (b) 730-nm, and (c) 740-nm excitations. Solid arrows are photon transitions, and dashed arrows are vibrational transitions.

determine with relatively high resolution the structure of the absorption spectrum of the Cr^{4+} ion in the spectral range where there is an overlap of features of both the Cr^{3+} and Cr^{4+} ions, that could not easily be resolved by standard absorption measurements.

EXPERIMENTAL RESULTS

The up-converted ordinary luminescence spectrum is shown in Fig. 2 for 532-nm laser excitation. The emission is characterized by a narrow peak due to the zero-phonon line at $\sim 26 450 \text{ cm}^{-1}$ followed by a broad vibrational side band peaking at $\approx 25 800 \text{ cm}^{-1}$. Attempts to fit this low-temperature emission spectrum using Pekarian band-shape curve yielded values of the Huang-Rhys parameter between $1 < S < 2$ and a phonon energy of $\sim 295 \text{ cm}^{-1}$. The 370-nm absorption band shown in Refs. 6 and 7 and its assignment using the Tanabe-Sugano energy diagram of Cr^{4+} doped forsterite suggests^{6–8} that this emission originates from the ${}^3T_1(t_2e)$ electronic state. The narrow peak at $\sim 26 450 \text{ cm}^{-1}$, corresponding to the zero-phonon transition, provides the exact position of this electronic state with respect to the ground state. This emission remains the same for laser excitations with wavelengths shorter than 578 nm, which is the cutoff wavelength for the ${}^3T_2 \rightarrow {}^3T_1(t_2e)$ transition [see Fig. 1(a)].

The lifetime of the ${}^3T_1(t_2e) \rightarrow {}^3A_2$ emission was measured using a streak camera operating in a synchroscan mode. The forsterite crystal which was held at liquid-nitrogen temperature was excited by a train of 55-ps, 532-nm pulses at a repetition rate of 82 MHz with an average power of 1.8 W from a frequency-doubled Nd:YAG laser. The lifetime was measured to be 395 ± 9 ps. The temporal profile of this emission is shown as an inset in Fig. 2.

Using the same excitation source (532 nm) but with increased spectral resolution (using a grating with 1800 grooves/mm) it was determined that the peak at $\sim 26 450$

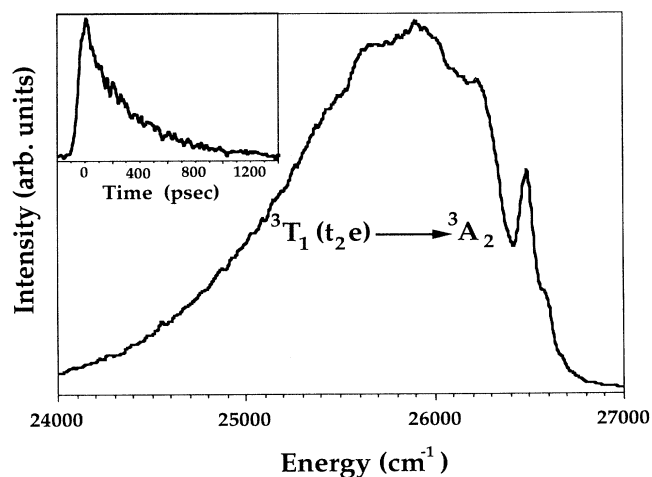


FIG. 2. Up-converted ordinary luminescence under 532-nm laser excitation. This emission arises from the ${}^3T_1(t_2e)$ state following excited-state absorption. The inset shows the temporal profile of this emission.

cm^{-1} actually consists of a zero-phonon line at $26\,424\text{ cm}^{-1}$ with two satellites at $26\,529$ and $26\,625\text{ cm}^{-1}$. The relative intensities of the three peaks were measured at several temperatures, and were shown to obey the Boltzmann distribution, indicating that they correspond to the same center. These three lines are assigned to the spin-orbit-split ${}^3T_1(t_2e)$ state of the tetrahedral Cr^{4+} ion. The emission spectra in the $26\,200$ – $26\,800\text{-cm}^{-1}$ range at two different temperatures are shown in Fig. 3.

The excitation spectrum of the ${}^3T_1(t_2e)$ state was obtained by measuring the integrated luminescence intensity over the 370 – 410-nm range as a function of the two-step excitation energy. This excitation spectrum is shown in Fig. 4 and is characterized by two peaks, one at $26\,425 \pm 10\text{ cm}^{-1}$ and another at $26\,525 \pm 10\text{ cm}^{-1}$. These two energies are the same as those of the two peaks observed in the up-converted luminescence spectrum. Since the pump wavelength was changed from 572.7 to 594.5 nm and assuming a two-step process, the effective excitation energy was determined by adding $\sim 9150\text{ cm}^{-1}$ to the energy of the excitation light covering effectively the $25\,970$ – $26\,610\text{-cm}^{-1}$ range. The third peak that could be expected at $26\,625\text{ cm}^{-1}$ was not observed because that energy was not available due to limited tuning range of the pump laser with a lower limit of 572.7 nm or, through an up-conversion process, $26\,610\text{ cm}^{-1}$. The excited-state absorption originates from the spin-orbit-split 3T_2 state, where the energies of the three levels are 9137 , 9151 , and 9169 cm^{-1} , as determined by Jia *et al.*⁸ Since the splitting is relatively small, and since the Boltzmann distribution for $T=78\text{ K}$ predicts that the relative populations of the three levels are reasonably close, an average

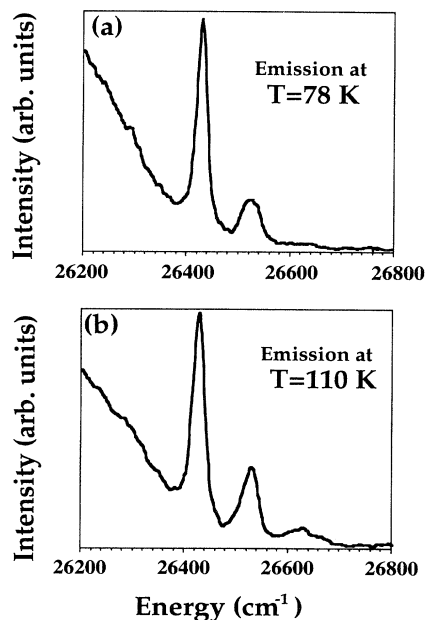


FIG. 3. High-resolution up-converted luminescence spectra for (a) sample temperature $T=78\text{ K}$, and (b) $T=110\text{ K}$. The three peaks correspond to the spin-orbit splitting of the ${}^3T_1(t_2e)$ state. The relative intensities of the three peaks obey the Boltzmann distribution.

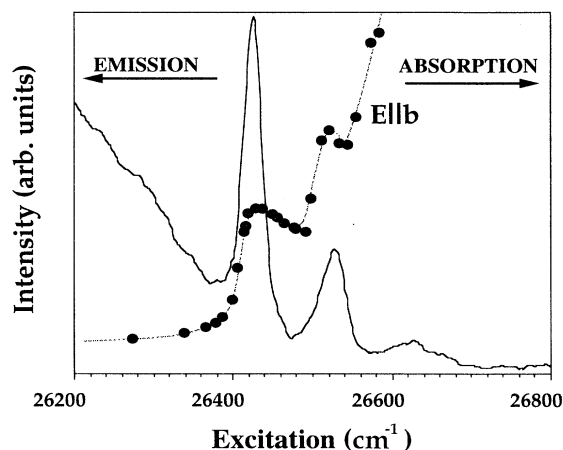


FIG. 4. Excited-state excitation spectrum: The integrated emission in the 378 – 414-nm spectral range is shown as function of the effective excitation (see text).

of 9150 cm^{-1} was used to calculate the effective excitation energy. The effect of the $\sim 30\text{-cm}^{-1}$ splitting of the SL was seen as a broadening of the features observed in the excited-state excitation spectrum. Nevertheless, the slightly broader structures observed in the excitation spectrum coincide with the sharp structures observed in the up-converted luminescence spectra, and unambiguously confirm that they correspond to transitions involving the same triplet excited state. The direct excitation spectrum of the ${}^3T_1(t_2e)$ state from 3A_2 was not measured because it required a tunable, narrow spectral width light source in the violet and near-ultraviolet spectral regions which was not available.

For photon energies lower than the energy of $17\,300\text{ cm}^{-1}$ required for the excited ion in the SL (2T_2) to reach the ${}^3T_1(t_2e)$ electronic state through the ESA process, a much weaker emission is observed. The interesting feature of this emission, shown in Fig. 5, is that it shifts when the laser wavelength is changed. The

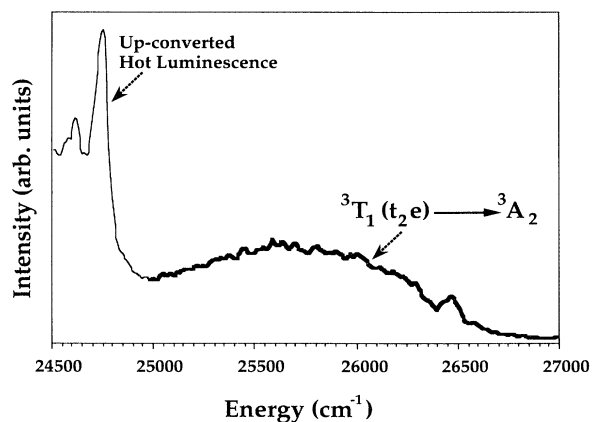


FIG. 5. Up-converted luminescence under 642-nm laser excitation. The higher-energy part (thick line) is due to the ${}^3T_1(t_2e) \rightarrow {}^3A_2$ emission following ESA from the ${}^3T_1(t_2e)$ state. The lower-energy part (thin line) is due to up-converted hot luminescence following ESA from the 3T_2 state.

highest energy peak is always at an energy level equal to E_{EL} in Eq. (1). These features are consistent with up-converted HL where the first peak is due to radiative transitions from the excitation level. The details of the experiments and analysis are presented elsewhere.¹⁹ For laser wavelengths longer than 600 nm there is not enough photon energy for the excited ions in the 3T_2 state to reach the ${}^3T_1(t_2e)$ metastable level by ESA. However, as shown in Fig. 5, the ${}^3T_1(t_2e) \rightarrow {}^3A_2$ emission is still present under 642-nm excitation, which indicates that ESA originates from another metastable level. [As will be shown below this metastable state is identified to be the ${}^3T_1(t_2^2)$ state of the Cr^{4+} ion.] The narrow peak at 26450 cm^{-1} and the broad sideband centered at 25800 cm^{-1} are identical to the features of the emission under 532-nm excitation shown in Fig. 2. Another narrow peak at 24740 cm^{-1} is the highest-energy peak in the up-converted HL spectrum ($E_{ph} + E_{SL}$).¹⁹ This [${}^3T_1(t_2e) \rightarrow {}^3A_2$] emission persists for laser wavelengths up to 730 nm. Figure 6 shows that this emission disappears under 740-nm excitation, which indicates that another metastable level exists such that ESA absorption from this level leads to population of the ${}^3T_1(t_2e)$ metastable level. This process is depicted in Figs. 1(b) and 1(c), respectively. The lifetime of this level should be longer than 12 ns since ESA is possible under our excitation conditions. The fact that the emission disappears under 740-nm excitation indicates that the energy gap between the newly identified metastable level and the ${}^3T_1(t_2e)$ state is slightly larger than the energy of the 740-nm photons. The cutoff wavelength of $735 \pm 5\text{ nm}$ can be used to estimate the energy (E_0) of this level (see Fig. 1):

$$E({}^3T_1(t_2e)) = E_0 + E(735 \pm 5\text{ nm}), \quad (2)$$

which yields

$$E_0 = 12\,847 \pm 90\text{ cm}^{-1}.$$

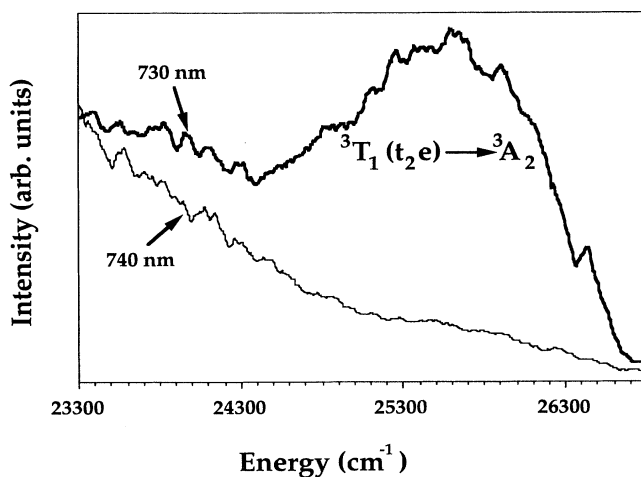


FIG. 6. The ${}^3T_1(t_2e) \rightarrow {}^3A_2$ emission under 730- and 740-nm excitation. This emission disappears under 740-nm laser excitation.

According to the Tanabe-Sugano energy-level diagram, the metastable state at energy E_0 is assigned to the ${}^3T_1(t_2^2)$ electronic state. More specifically, taking into account the splitting of the ${}^3T_1(t_2^2)$ state due to orthorhombic distortion of the tetrahedron containing the Cr^{4+} ion,⁸ this level is the lowest vibronic level of the ${}^3A_2({}^3T_1)$ state.

DISCUSSION

The ratio of the intensities of the ${}^3T_1(t_2e) \rightarrow {}^3A_2$ transition after ESA originating from the 3T_2 SL (laser wavelength shorter than 570 nm) over the intensity of the emission following ESA from the ${}^3T_1(t_2^2)$ state (laser wavelength longer than 600 nm) is of the order of 100. This means that the average population of the ${}^3T_1(t_2^2)$ state is approximately 10^{-2} the population of the 3T_2 SL, assuming the same cross sections. Therefore, knowing the lifetime of the 3T_2 state of $2.7\ \mu\text{s}$, the lifetime of the ${}^3T_1(t_2^2)$ state should be of the order of hundreds of nanoseconds. The ${}^3T_1(t_2^2)$ state exhibits strong absorption for all crystal orientations. Ordinary luminescence from the ${}^3T_1(t_2^2)$ state [beginning at 780 nm and longer according to Eq. (2)] has not been detected because of the presence of Cr^{3+} ions in forsterite that emit very strongly in the same spectral region. Another reason could be the relatively weak emission intensity due to the short lifetime of the ${}^3T_1(t_2^2)$ state. An attempt was made to observe the ${}^3T_1(t_2e) \rightarrow {}^3T_2$ transition. This emission is expected to have a similar spectral profile to the ${}^3T_1(t_2e) \rightarrow {}^3A_2$ emission due to the very small offset between the ground state (3A_2) and the 3T_2 state, as indicated by the Huang-Rhys parameters $S < 1$.^{19,20} The zero-phonon peak is expected at $\approx 570\text{ nm}$. Using 532-nm laser excitation, the 570-nm spectral region is occupied by the Raman signal which is much stronger. Pumping with 457.9 nm from an argon-ion laser to avoid the Raman signal, the emission observed at the 570-nm spectral region was approximately 50 times stronger than the observed ${}^3T_1(t_2e) \rightarrow {}^3A_2$ transition, and no structure with the expected characteristics was detected.

The same experiments were attempted on a forsterite crystal grown in a reducing atmosphere favoring Cr^{3+} substitution, but none of the above emission spectra were observed. This indicates that the reported emissions are due to Cr^{4+} ions. The intensity of the up-converted OL changes as the square of the average laser excitation power. However, no change in the intensity was observed when the pulsewidth was varied, keeping the average power constant. This intensity dependence is consistent with radiative transitions following excited-state absorption.

The overall up-converted emission under 532-nm laser excitation in the $24\,000\text{--}28\,000\text{ cm}^{-1}$ spectral region can be divided into two sectors (A and B in Fig. 7) of very different intensity. Sector B is due to the ${}^3T_1(t_2e) \rightarrow {}^3A_2$ transition that is also shown in Fig. 2. Sector A is due to up-converted hot luminescence from the very short-lived vibronic levels populated during the relaxation of the photoexcited ions by phonon emission.¹⁹ The first narrow peak in the up-converted hot luminescence spectrum

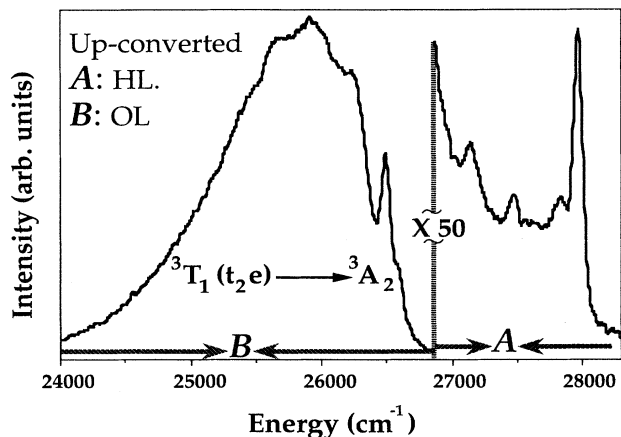


FIG. 7. Up-converted luminescence under 532-nm excitation. Section A is due to up-converted hot luminescence. Sector B is due to ordinary luminescence from the ${}^3T_1(t_2e)$ electronic state. The sample was held at liquid-nitrogen temperature.

is located at $27956\text{ cm}^{-1} = h\omega_{532\text{nm}} + E_{\text{SL}}$. The lifetime of the ${}^3T_1(t_2e)$ electronic state was measured to be 395 ps. The integrated intensity of ${}^3T_1(t_2e) \rightarrow {}^3A_2$ emission (B) sector is estimated to be ≈ 600 times stronger than the emission from the highest-energy vibronic level (first

narrow peak in up-converted HL emission in sector A) under the same 532-nm laser excitation. The ratio of intensities due to emission from different levels of the same electronic state should be equal to the ratio of their lifetimes.¹⁸ Therefore, the lifetime of the highest-energy vibronic level is estimated to be ~ 660 fs (395 ps/600). Since the depletion of the population of a nonequilibrium vibronic state is due to the emission of phonons during the vibrational relaxation of the excited ions, this time can also be considered as the time between successive phonon emission in this part of the excited state manifold.

In summary, up-converted luminescence and excited-state excitation spectroscopy were used to obtain information about the energy structure of Cr^{4+} forsterite that could not be obtained using standard absorption and luminescence techniques. The presence of two additional metastable levels is indicated, and their energy is determined. The three levels of the spin-orbit-split ${}^3T_1(t_2e)$ state are located at 26424, 26529, and 26625 cm^{-1} and the ${}^3T_1(t_2^2)$ state is at 12847 cm^{-1} .

ACKNOWLEDGMENTS

We thank Dr. R. Guenther for technical discussions. The research is supported by the Army Research Office, Grant No. DAAL03-91-G-0066.

- ¹V. Petričević, S. K. Gayen, R. R. Alfano, K. Yamagishi, H. Anzai, and Y. Yamaguchi, *Appl. Phys. Lett.* **52**, 1040 (1988).
- ²V. Petričević, S. K. Gayen, and R. R. Alfano, *Appl. Phys. Lett.* **53**, 2590 (1988).
- ³H. R. Verdun, L. M. Thomas, D. M. Andrauskas, T. McCollum, and A. Pinto, *Appl. Phys. Lett.* **53**, 2593 (1988).
- ⁴V. G. Barishevskii, M. V. Korzhik, A. E. Kimaev, M. G. Livshitz, V. B. Pavlenko, M. L. Meilman, and B. I. Minkov, *Zh. Prikl. Spektrosk. (Moscow)* **53**, 7 (1990) [*J. Appl. Spectrosc. (Moscow)* **53**, 675 (1990)].
- ⁵A. Seas, V. Petričević, and R. R. Alfano, *Opt. Lett.* **16**, 937 (1992).
- ⁶V. Petričević, S. K. Gyen, and R. R. Alfano, in *Tunable Solid-State Laser*, OSA Proceedings Series Vol. 5, edited by M. L. Shand and H. P. Jenssen (Optical Society of America, Washington, D.C., 1989), pp. 77–84.
- ⁷H. R. Verdun, L. M. Thomas, D. M. Andrauskas, T. McCollum, and A. Pinto, in *OSA Proceedings of the Advanced Solid-State Lasers*, edited by M. L. Shand and H. P. Jenssen (Optical Society of America, Washington, D.C., 1989), Vol. 5, p. 85.
- ⁸W. Jia, H. Liu, S. Jafe, and W. M. Yen, *Phys. Rev. B* **43**, 5234 (1991).
- ⁹R. Moncorge, G. Cormier, D. J. Simkin, and J. A. Capobianco,

- J. Quantum Electron.* **27**, 114 (1991).
- ¹⁰K. R. Hoffman, J. Casas-Gonzales, S. M. Jacobsen, and W. M. Yen, *Phys. Rev. B* **44**, 12589 (1991).
- ¹¹K. Peuker and E. D. Trifonov, *Phys. Status Solidi* **30**, 479 (1968).
- ¹²V. Hizhnyakov and I. Tehver, *Phys. Status Solidi* **39**, 67 (1970).
- ¹³Yuzo Mori, Ryo Hattori, and Hiroshi Ohkura, *J. Phys. Soc. Jpn.* **51**, 2713 (1982).
- ¹⁴Y. Kondo, T. Noto, S. Sato, and M. Hirai, *J. Lumin.* **38**, 164 (1987).
- ¹⁵E. W. J. L. Oomen, *J. Lumin.* **50**, 317 (1992).
- ¹⁶A. Silversmith, W. Lenth, and R. M. Macfarlane, *Appl. Phys. Lett.* **54**, 2301 (1989).
- ¹⁷R. Moncorge, F. Auzel, and J. M. Breteau, *Philos. Mag. B* **51**, 489 (1985); R. Moncorge and T. Benyattou, *Phys. Rev. B* **37**, 9186 (1988).
- ¹⁸S. G. Demos, and R. R. Alfano, *Phys. Rev. B* **46**, 8811 (1992).
- ¹⁹K. R. Hoffman, S. M. Jacobsen, J. Casas-Gonzalez, and W. M. Yen, in *OSA Proceedings of the Advanced Solid-State Lasers*, edited by G. Dubé and L. Chase (Optical Society of America, Washington, D.C., 1991), Vol. 10, p. 44.
- ²⁰B. Henderson and G. F. Imbusch, *Optical Spectroscopy of Inorganic Solids* (Wiley, New York (1989), Chaps. 5 and 9.